Proceedings of the 7th International Symposium on Cavitation
CAV2009
August 16-20, 2009, Ann Arbor, Michigan, USA

CAV2009 – Paper No. 8

Numerical Analysis of Hydrofoil Ventilated Cavitation under Wave Impact

E. L. Amromin
Mechmath LLC
Prior Lake, MN55372, USA

ABSTRACT

Unsteady ventilated cavitation of a hydrofoil is analyzed with coupling of the perturbed steady two-dimensional incompressible flow of water out of the cavity and the compressible one-dimensional air flow within the cavity. The air flux from cavity at its oscillating tail and along its side boundary with the water is taken into account. The employed equations include air mass conservation law and pressure constancy condition along the cavity in both media. On the cavity boundary, however, the impermeability condition is considered from the water side and the differential momentum equation from the air side.

The developed model of ventilated cavitation has been verified with the already published [1] measurements of hydrodynamic loads and their pulsations on the low-drag partially cavitating hydrofoil OK-2003. A satisfactory agreement of the computed results with experimental data was manifested. Influence of the wavelength variations and air compressibility on lift and its pulsations were analyzed.

INTRODUCTION

For many decades ventilation has been widely used in experiments on cavitation (since [2]) and in the drag reduction by cavitation (since [3]). A substantial coupling of the gas flow within the cavity with the water flow out of the cavity is the well known fact. The recent experiments [1] with the ventilated hydrofoil OK2003 (shown in Fig.1) also manifested this. Although this coupling exists in both steady and unsteady flows, an analytical study of wave impact on ventilated cavities is practically more urgent than such a study for steady flows (as described in [4]) because experiments with wavy flows are more complex technically and generally are much more expensive. Moreover, this coupling is especially significant for cavitation in unsteady flows because the cavity response on unsteady perturbations by the water flow must qualitatively depend on the air compressibility (dislike to cavitation in steady flows). Nevertheless, this coupling is a quite new topic.

An unsteady ventilated cavity under the wave impact is considered here as the perturbed steady cavity in ideal fluid. As usual in ideal fluid theory, the flow is determined with the velocity potential $\Phi(x,y,t) = \Phi_0(x,y) + \Phi^*(S,t) + \varphi(S^*,t)$ that is here a sum of solutions of the time-independent nonlinear problem and two time-dependent linear problems.

The potential $\Phi_0(x,y)$ describes flow around a hydrofoil (body) with the steady unperturbed cavity. The surface S* of this cavity and the velocity distribution U =gradΦ over all flow boundaries become known from the solution of the following nonlinear steady problem for the velocity potential Φ_0 :

$$\Delta\Phi_0 = 0; \quad \left.\frac{\partial\Phi_0}{\partial N}\right|_S = 0; \quad \left. U^2 \right|_{S^*} = 1 + \sigma \qquad (1)\text{-}(3)$$

Here the first equation is the water mass conservation law. The second equation is the impermeability boundary condition on the surface S that includes S* and the wetted body surfaces. The third equation is the pressure constancy condition for the cavity. There is no any consideration of flow within the cavity in Eq.(1)-(3) and one may say that an empty cavity concept is used there. Nevertheless, numerous comparisons (from [5]) of this concept with experimental data on ventilated cavities in steady flows confirm its acceptability to them.

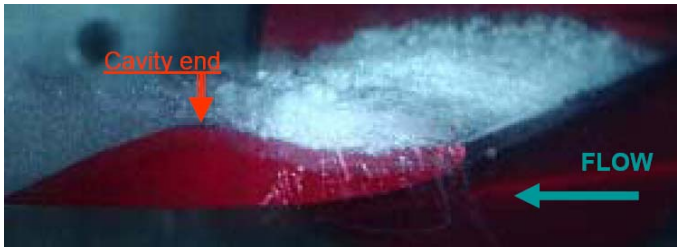

Figure 1: View of the hydrofoil OK2003 with ventilated cavity in the suction side concavity

The potential Φ*(S, t) describes unsteady perturbations on the surface S determined by solving the problem (1)-(3). Φ* does not take into account cavity deformations under impact of perturbation and must be found by solving the problem

$$\Delta\Phi^* = 0; \quad \partial\Phi^* / \partial N\big|_S = -v(t,x); \quad \frac{d}{dt}\int \Gamma dl = 0; \qquad (4)\text{-}(6)$$

Integration in Eq.(6) is made around the hydrofoil and along its wake Sw. Unlike to the problem (1)-(3), this boundary value problem does not include the pressure constancy condition.

The problem (4)-(6) is a linear problem. Let us show that such a perturbation approach allows a satisfactory determination of pulsating loads. The comparison of computed with Sw directed along average incoming flow speed and measured [6] pressure pulsation along a cavitation-free hydrofoil is given in Fig.2. The agreement of computation with measurement is good enough.

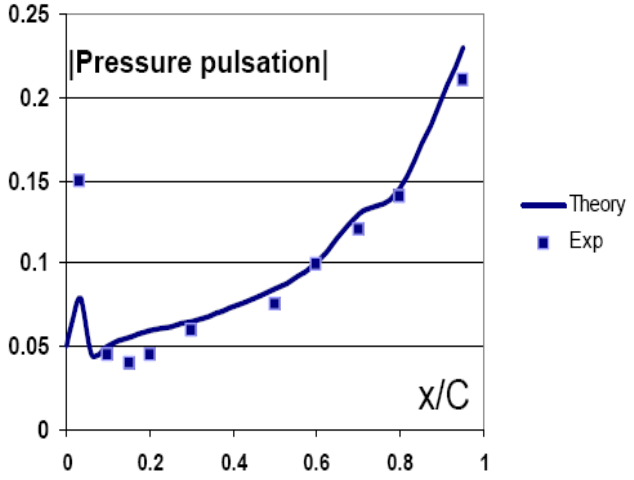

Figure 2: Computed and measured dimensionless pressure pulsation on the foil NACA0012 in gust flow of a wind tunnel.

The potential φ(S*, t) describes velocities caused by the cavity surface deformation. It is assumed here that the derivatives of φ are much smaller than U_∞ is and the cavity thickness variation h (shown in Fig.3) is much smaller than the cavity length is. Such assumptions allow quasi-linearization of the boundary conditions for the potential φ.

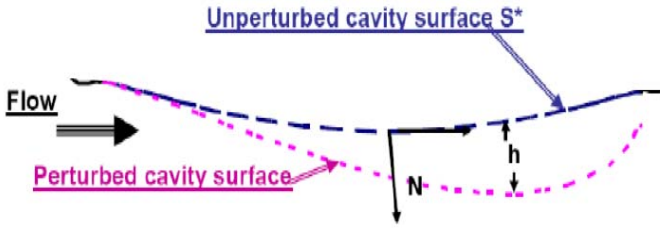

Figure 3: Sketch of cavity perturbed boundary

The following analysis is emphasized on determination of cavity perturbations and time-depending forces. Unlikely to the problem (1)-(3), the air flow within the cavity will be taken into account in this analysis.

EQUATIONS FOR CAVITY PERTURBATIONS

Let us neglect by products of assumingly small quantities. The water pressure P in the unsteady perturbed flow (with incoming perturbation potential ψ) is then defined as following:

$$\frac{P}{\rho_w} + \frac{\left|grad(\Phi_0 + \Phi^* + \psi + \varphi)\right|}{2} + \frac{\partial(\psi + \Phi^* + \varphi)}{\partial t} = \frac{P_\infty}{\rho_w} + \frac{U_\infty^2}{2}$$

Defining φ as the source-sink potential of a small intensity q and Φ* as the potential depending on both small source-sink intensity q* and small vortex perturbed intensity γ, one can determine γ with Eq.(6) and q* with Eq.(5).

The function q can be determined with condition on the cavity surface only. Taking into account the air compressibility in the cavity and assuming that the same time-depending pressure P(t) is instantly settled in the whole cavity, one can write the pressure constancy condition within the cavity as

$$\frac{U}{2\pi}\int \frac{qd\xi}{x-\zeta} + \frac{1}{2\pi}\int \frac{\partial q}{\partial t}\ln|x-\zeta|\,d\xi + \frac{U}{2\pi}\int_{(Sw)} \frac{(T,[\gamma,R])}{R^2}d\zeta +$$

$$+\frac{d}{dt}\int_0^x \gamma d\zeta + \rho' J = -Uu' - \frac{\partial\Phi^*}{\partial t} \qquad (7)$$

Here the parameter $J = \rho_0 c^2 / \rho_w U_\infty^2$ substantially depends on air concentration in the mixture filing the cavity (see Fig.4).

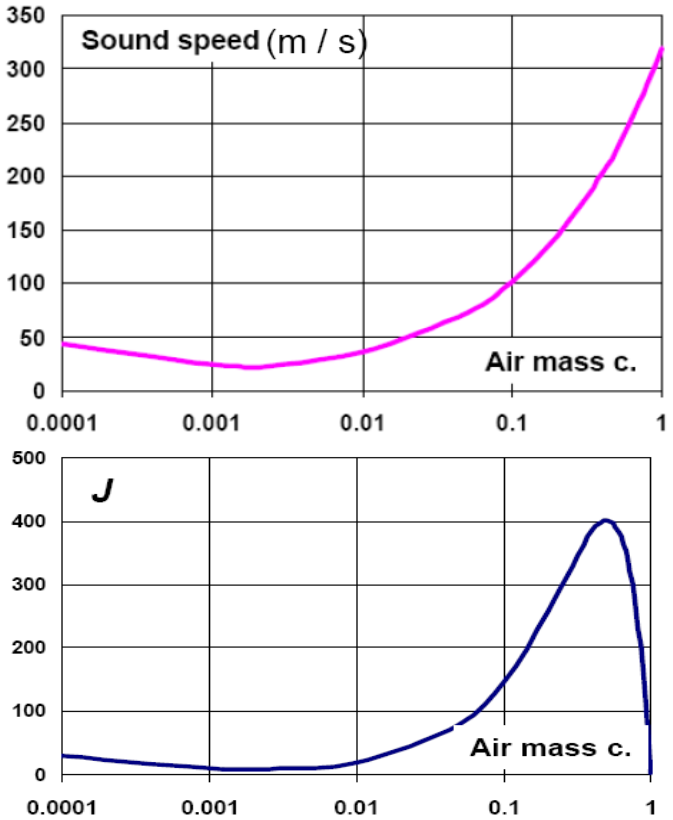

Figure 4: Sound speed versus air mass concentration in the air-water mixture within the cavity (top) and value of the parameter J versus this concentration for the free-stream speed 8m/s (bottom)

The mixture sound speed for this plot was calculated with employment of following definitions [7]:

$$\frac{1}{\rho}=\frac{m}{\rho_0}+\frac{1-m}{\rho_W},\qquad c=\sqrt{dP/d\rho}$$

Here ρ is the mixture density. The sound speed in water is practically constant in conditions considered here.

Determination of the density variation ρ' requires estimate the air escape from cavity. There are two ways of this escape: One way goes through the cavity side surface into the water boundary layer on the cavity, another way goes through the cavity oscillating tail. The one-dimensional mass conservation law for the cavity can be written in perturbations as

$$V\frac{\partial\rho'}{\partial t}+\int_0^{l_C}\frac{\partial h}{\partial t}dx=Q-Q_{sm}-\max\left\{0,\ hu_a\Big|_{x=l_C}\right\} \quad (8)$$

The first term in the left-hand of this equation describes the mass variation due to the air density perturbation, whereas the second term describes its variation due to oscillation of the cavity volume. The third term in the right-hand side of Eq.(8) describes the air escape through the cavity tail.

The cavity deformation in Eq.(8) can be expressed through the intensity q by using the perturbed impermeability boundary condition on the cavity

$$\frac{q}{2}=\frac{\partial(Uh)}{\partial x}+\frac{\partial h}{\partial t} \quad (9)$$

However, an equation for the function u_a from Eq.(8) is necessary yet. It was recently found [8] that the air mixing with the cavity boundary layer substantially depends on turbulent mixing. Therefore, Prandtl equation as the simplest form of momentum equation in turbulent flow is considered here on S*:

$$\frac{\partial u_a}{\partial t}+\frac{\partial(u_a^2)}{2\,\partial x}=-\frac{aU^2}{H+h} \quad (10)$$

Here the empirical Clauser constant ***a*** may be tuned with experimental data on the wave-free flows.

Adequacy of Eq.(10) to the ventilation problem can be estimated with an example of steady ventilation in a niche of depth H. For this example of the cavity with no tail pulsation ($u_a\big|_{x=l_C}=0$), the solution $u_a=\sqrt{u_{a0}^2+2aU^2x}$ of Eq.(10) will be transformed into the formula $Q_{sm}/b=\sqrt{2al_cHU}$, where b is the niche width. This gives Q_{sm} scaling with the power 5/2 and just such law was mentioned in [9] for ships with bottom drag reduction by ventilation.

Thus, it is sufficient to solve Eq.(7)-(10) for determination of four functions q(x,t), h(x,t), u_a (x,t) and ρ'(t). However, the cavity perturbations are limited by the hydrofoil concavity surface. Therefore, taking into account that the unperturbed cavity thickness H>0 and the positive values of the perturbation h are counted below the unperturbed cavity surface, one should write the corresponding limitation in the form of condition

$$h(x,\tau)+H(x)\ge 0 \quad (11)$$

The time-dependent condition (11) is the cause of the multi-frequency cavity response on one-frequency excitations in this approach to unsteady problems (the dimensionless time τ is further used in all computations and plots of this paper).

It is also important to point out here that, unlikely to majority of ventilated hydrofoils (described in [10] and [11], for example) the ventilated hydrofoil OK-2003 has very stable cavities with insignificant cavity tail pulsation and drag pulsations at the design conditions (for the angle of attack of 6 degrees, these conditions correspond to 0.95<σ<1.0, as shown in Fig.5; the air fills the suction side concavity only at σ<1.0). For these conditions, both drag and lift pulsation fall below their values for the same cavitation-free hydrofoil. Therefore, it is possible to assume $h(l_C,t)=0$ for perturbation-free situations.

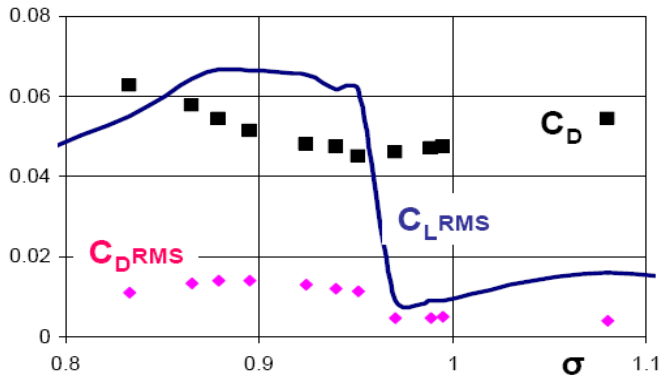

Figure 5: Measured dependencies of coefficients of drag, lift and drag RMS on cavitation number for ventilated hydrofoil OK-2003 in steady flow at 6 degree angle of attack (after [1]).

LIFT DETERMINATION

The unsteady lift is computed by direct integration of pressure and the time-average value of C_L is then calculated by direct averaging. This value is generally different [1] from C_L in steady flow at the same angle of attack, but it is important to correctly determine such C_L because distribution of U employed in computation of unsteady pressure depends on C_L.

There is, however, the well-known issue in computation of the steady C_L for partially cavitating hydrofoils. As summarized in [12], the closed cavity schemes with Kutta-Joukowski condition for lift determination overestimate C_L for large partial cavities. Moreover, the significant fraction of the real range of σ occurs out of consideration (as shown in Fig.6 with experimental data [13]).

Open schemes can give quite realistic lift coefficients, $C_L(\sigma)$, but the cavity length in these schemes is usually 60-70% of the measured time-average values. For ventilated hydrofoils, both the cavity size and the hydrodynamic loads are important as information. On the other hand, the realistic lift behavior in open schemes looks to be associated by replacement of the Kutta-Joukowski condition with another that would be more suitable for flows with large partial cavities. A successful replacement of this condition for a closed cavity scheme was done [14] with assumption that the lift difference for cavitating and cavitation-free flows is caused by pressure change under the cavity itself only:

$$C_L(l_c) = C_L(0) + \int_{X_1}^{X_1+l_c} [1 + \sigma - U^{*2}(x)]dx \qquad (12)$$

Here U* is computed for the cavitation-free flow with the Kutta-Joukowski condition (such a correction to the lift may be simulated by a vortex distribution along the cavity). The successful employment of the above lift correction for 2D problems is illustrated by Fig.6 for the EN-hydrofoil and by Fig.7 for the OK-2003 hydrofoil.

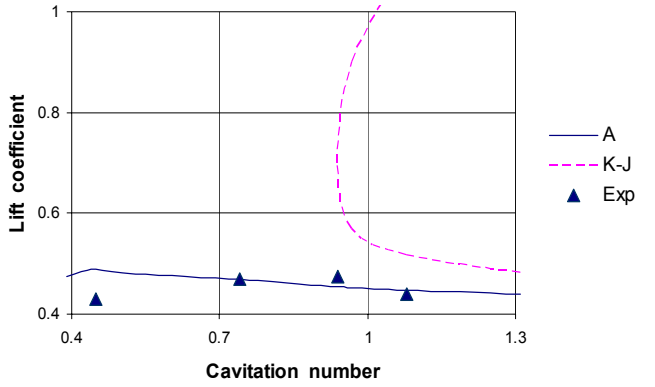

Figure 6: Comparison of theory and experiment for the EN-hydrofoil at α=4.2° with partial cavitation. The line K-J shows computation with a closed scheme and Kutta -Joukowski condition. The line A shows computations with Eq.(13).

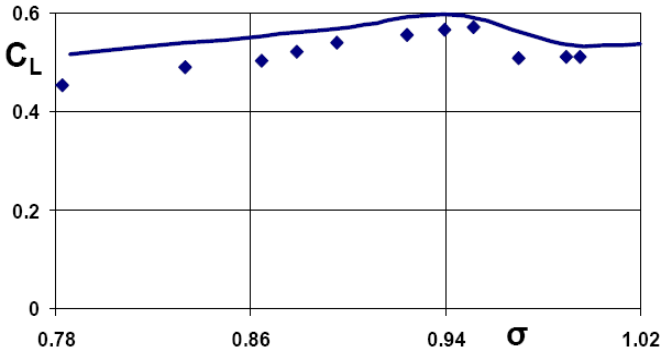

Figure 7: Lift coefficient of the ventilated hydrofoil OK-2003 in steady flow at 6 degrees (after [1]). The air supply rate is 5liter/minute, C=81mm, free-stream speed is 8m/s. Rhombs show measured data. The curve gives the described theory results.

For the small hydrofoil in the water tunnel, wall blockage augments the lift, whereas on the other hand, there is also a significant Reynolds number effect leading to the lift decrease. The bias to experimental data to take into account both effects in the provided steady flow computations for the hydrofoil OK-2003 was gotten: The angles of attack for the computed unbounded flow of ideal fluid were tuned to the values giving the same lift coefficients with the cavitation-free flow in the water tunnel.

MORE DETAIL ON COMPUTATIONS

The iterative technique for solving nonlinear steady problem (1)-(3) is well developed. Its descriptions may be found in many papers (from [15] to [14]). Its solution gives U for Eqs.(7)-(11), whereas the initial values h(S*)=0, q(S*)=0,γ(Sw)=0 and q*(S)=0 are ordered at τ=0.

Unsteady quasi-linear problems (4)-(6) and (7)-(10) are much more time-consuming than the steady nonlinear problem is. However, solving Eq.(4)-(6) and the consequent calculation of the functions $u'(S,t), \partial\Phi^*(S,t)/\partial t$ for Eq.(8) can be reduced to multiplication of a preliminary computed time-independent matrix and a time-dependent vector combined from values of the right-hand side of Eq.(5). Employing a BEM technique and representing Eqs.(5) as an integral equation, one can transform it to a linear algebraic system and rewrite it into the matrix equation $B\bar{q}^* + D\bar{\gamma} = -\bar{v}$, where matrixes B and D are time-independent and the values of γ are determined with Eq.(6), but variation of the vortex intensity along the hydrofoil chord differs from the variation corresponding to Kutta-Joukowski condition by the factor $r = C_L(l_c)/C_L(0)$. The velocity $u' = \partial(\Phi^* + \psi)/\partial T$ can then be represented with matrixes as

$$\bar{u}' = F\bar{q}^* + \bar{\psi}^* = \bar{\psi}^* - FB^{-1}D\bar{\gamma} - FB^{-1}\bar{v} \qquad (13)$$

Similar presentations as of products of the time-independent matrixes and time-dependent vectors can be employed for $\partial(\Phi^* + \psi)/\partial t$, derivatives of φ and for h(x,t). Such presentations reduce the number of arithmetic operations **m** at any time step down to **m**~**n**^{2}, where **n** is number of boundary elements (in comparison with **m**~**n**^{3} for an algorithm without preliminary matrix calculation, the employed algorithm gives approximately hundredfold computer time saving). Further, $\partial(\Phi^* + \psi)/\partial t$ is represented as the derivative of an integral of u$'$ with employment of matrixes already computed for Eq.(13).

Generally, there is the possibility to take into account the water tunnel wall existence in the problem (1)-(3) by their including in S. However, particularly for this analysis, their influence has been first taken into account by the above-mentioned bias in the lift determination and by correction of the cavitation number (with the for free-stream speed corrected on water tunnel blockage by the same cavitation-free hydrofoil). Additionally, the wall effect must be taken into account in calculating the contribution of sources q(x) to the pulsating water pressure.

As was mentioned, the coefficients {a, Q_{sm}} are taken here from the experiments on steady ventilation. The influence of Q on computational results is illustrated by Fig.8.

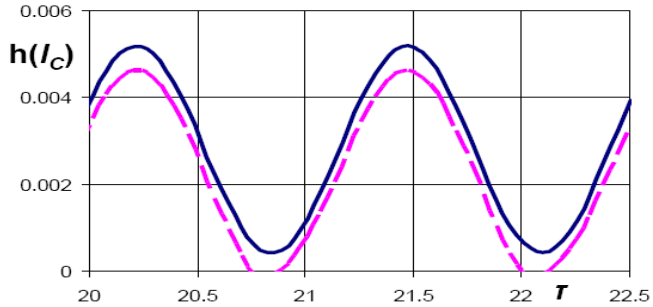

Figure 8: Influence of air supply Q on oscillations of the cavity tail under wave impact. Dashed curve relates to Q= Q_{sm}. Solid curve relates to Q=1.1Q_{sm}.

One can see that under the wave impact, it will be insufficient to keep the air supply necessary for maintaining smoothly closed cavity in the steady flow: The cavity periodically becomes shorter. On the other hand, a modest increase of air supply leads to a permanent air escape from the ventilated cavity through its tail. The equations (8)-(11) content partial derivatives in the plane {x, τ}. The second order schemes with approximation of these derivatives in the rectangle centers {x+dx/2, τ+dτ/2} have been employed here. The grid selection effect on computational accuracy is illustrated by Fig.9, where the lift coefficient variations with the dimensionless time τ are compared for different time steps.

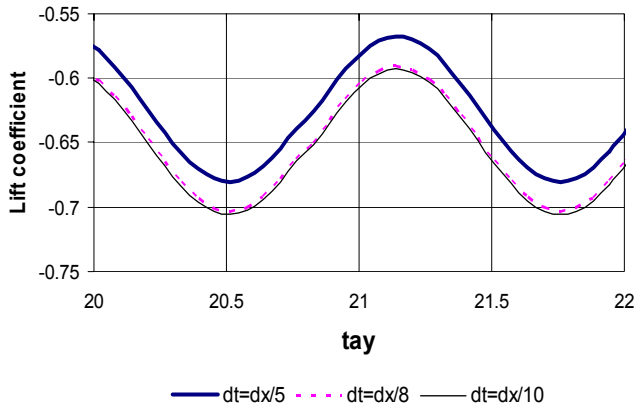

Figure 9: An example of influence of the time step on the computed instant lift coefficient.

The ratio dx/*lc*=1/50=10dτ has been employed in the computations provided below. Calculation of the averaged lift, lift RMS (and other averaged characteristics) has started at least after 10 periods of wave impact.

COMPARISON WITH EXPERIMENTAL DATA

The wavy (gust) flow impact experienced by the hydrofoil OK-2003 in the water tunnel of the Saint Anthony Falls Laboratory has been generated with a gust generator upstream of the hydrofoil (its description was given in [1].) The measured vertical wave-induced velocity component at the hydrofoil location can be approximated by the formula

$$v(x,t) = w + A\sin(2\pi x/\lambda - \omega t) \qquad (14)$$

Here $\lambda=U_\infty/(2\pi\omega)$. Another velocity component can be reconstructed from $\Delta\psi=0$. For the experiments with the hydrofoil OK-2003, the {w, A} values for different flap oscillation magnitudes β have been following:

Table 1: Gust parameters for Eq.(14)in water tunnel test [1]			
C/λ	**β (degrees)**	***w***	***A***
0.2	**2**	**0.0087**	**0.0174**
0.4	**2**	**0.0105**	**0.0218**
0.2	**4**	**0.0087**	**0.0349**
0.2	**4**	**0.0105**	**0.0446**

For the immobile flaps *W*=*w*=0.

Comparing computed forces on the ventilated hydrofoil in gust (wavy) flow with their measurements [1], one must recall that these measurements were not supplemented by the direct measurements of the cavity pressure Pc. It was supposed there that for a fixed water tunnel pressure, σ depends on Q and U_∞, but it does not depend on A and λ. Indeed, the waves affect the cavity pressure and, consequently, the cavitation number. However, as manifested by computational dependencies presented in Fig.10, the oscillations of cavitation number are not significant even for the cavities with significant water volume concentrations (J close to 20) and can be neglected in the comparisons of computations with experimental data.

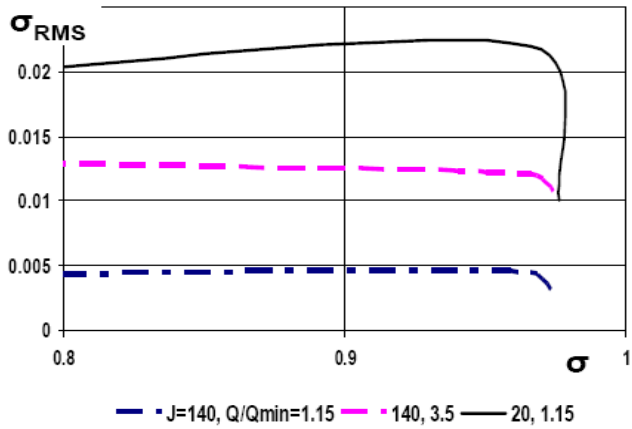

Figure 10: Influence of the parameter J (mixture compressibility in the cavity) and air supply on RMS of cavitation number at α= 6 degrees and λ=2.5C. Greater air flux amplifies pulsations.

Comparisons of the computed average lift coefficient in gust flow with its measurement [1] in Fig.11 shows a very good agreement of the theory with experimental data.

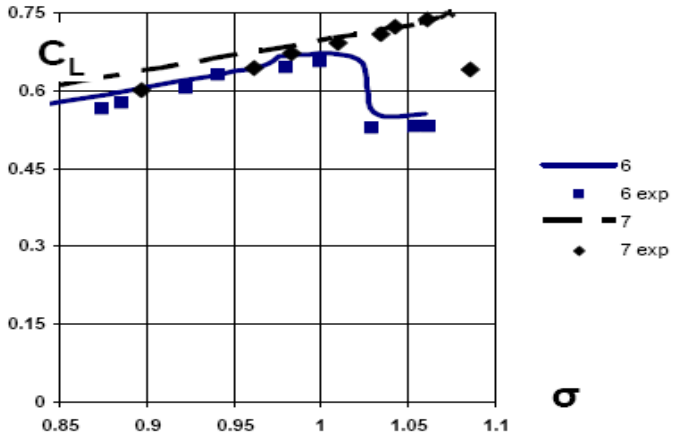

Figure 11: Comparison of computed (lines) and measured (symbols) average lift coefficient at λ=2.5C and defined by Eq.(14) wave magnitude A=πU/72

The agreement is not so good for the lift RMS in Fig.12. There are several possible causes for the greater discrepancies of the lift RMS. First of all, some lift pulsations are inherent to both the cavitation-free flow and cavitation in steady incoming flow; their level was shown in Fig.5 (for σ>1.05 at α=6°, there has been no steady ventilated cavitation in experiments [1]) whereas the potential φ describes only the wave-induced cavity perturbation.

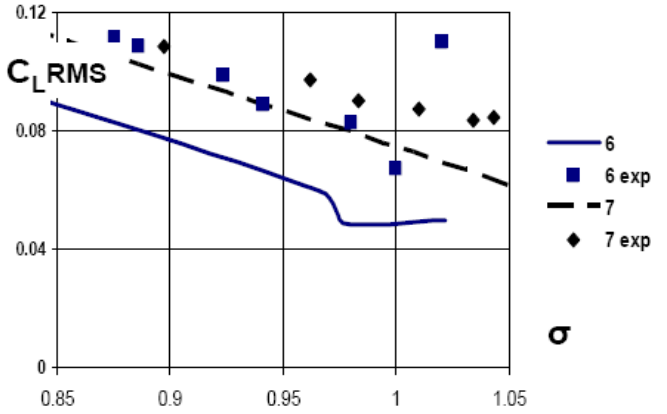

Figure 12: Comparison of computed (lines) and measured (symbols) RMS of lift coefficient at λ=2.5C and A=πU/72.

Attempting take into account other perturbations, one may assume that wave-induced perturbation can be excited manly at the frequency ω and its harmonics, whereas wave-independent perturbations (corresponding to A=0) significantly contribute to cavity pulsation at others frequencies only. The corrected coefficient $C_{LRMS} = \sqrt{C^2_{LRMS}(A) + C^2_{LRMS}(0)}$ can then be calculated with employment of $C_{LRMS}(0)$ from Fig.5. Comparing solid curves in Fig.13 with such coefficient in Fig.12, one can see that this correction reduces the discrepancy of theory with the experimental data.

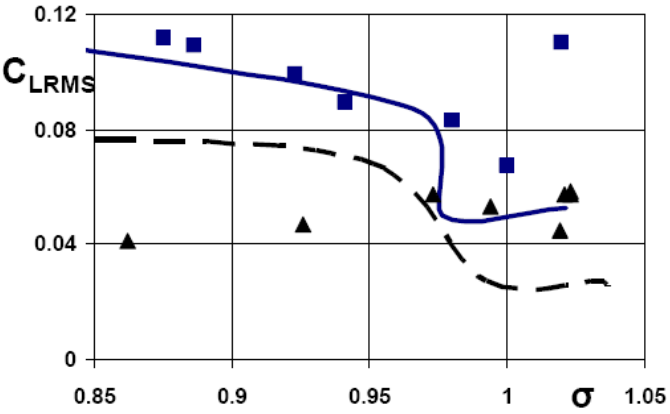

Figure 13: Comparison of computational dependencies for lift RMS coefficient defined as $\sqrt{C^2_{LRMS}(A) + C^2_{LRMS}(0)}$ with experimental data. Solid line (theory) and squares (measurements) relate to A=πU/72, λ=2.5C, α=6 degrees. Dashed line (theory) and triangles (measurements) relate to A=πU/144, the same λ and α.

This correction does not look uniformly good for the various wave magnitudes in comparison with experimental data, but these data themselves do not exhibit uniform trends and tendency to collapse with some simple normalization. Also, a modification of the suggested approach by replacing of the ideal fluid solution {U(x), H(x)} for unperturbed flow with some solution for cavitating flow of viscous fluid may be a reasonable alternative to employment of experimental data for $C_{LRMS}(0)$. Such alternative could make it possible to analyze also the drag pulsations (here no attempt of drag pulsation analysis was made because of supposedly dominant contribution of boundary layer effects to drag of this hydrofoil).

On the other hand, it is important to keep analyzing wave-induced loads on the basis of ideal fluid theory. Such analysis evidently saves the computer time. However, it is more important that such analysis gives the possibility to separate the Reynolds number-dependent characteristics from the Reynolds number-independent characteristics, as it is currently accepted in engineering practice and employed in scaling of the model test results, whereas even well-working RANS code does not help in scaling because of the mentioned issue with separation of two kinds of characteristics.

WAVELENGTH EFFECT

The experimental data [1] have been obtained also for the wavelength λ/C=5, but this λ was not used here because the distance between water tunnel walls practically coincides with the half of this wavelength. This coincidence certainly caused some resonances and the presented quasi-linear approach looks insufficient for such case.

The wavelength effect on the response of ventilated cavities is illustrated here by numerical examples. The sea waves are mainly waves of a small ratio of amplitude to wavelength and this ratio is quite close to a constant for a wide band of λ. Further, normalization was made with the value of lift RMS at design condition for λ=C. As expected, the maximum response occurs for the wavelength λ=C coinciding with the foil (body) longitudinal dimension. As shown in Fig.14, there is no significant difference in the lift RMS for ventilated hydrofoils for λ=C at the design and off-design conditions. However, the difference increases with the wavelength. For design condition, the λ increase over C leads to reduction of lift pulsations, whereas this increase has the opposite effect for the off-design conditions.

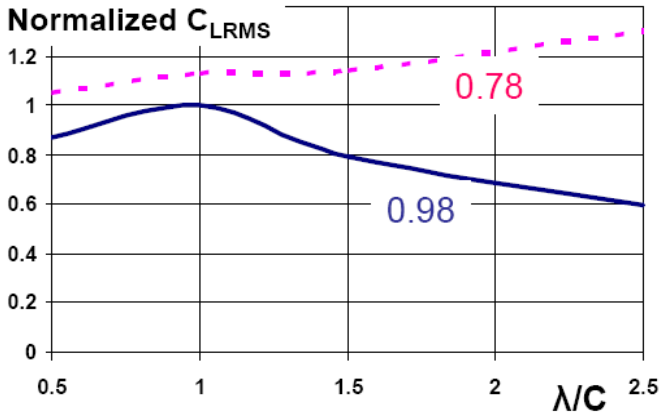

Figure 14: Wavelength effect on normalized lift RMS for α=6° and a constant ratio of wave magnitude to wavelength in design condition (σ=0.98) and off design condition (σ=0.78).

The wavelength effect on the average lift is significant only at off-design conditions. As shown in Fig.15, such effect

also significantly depends on the air supply ratio (here Q_{sm}=4.3L/min, as it was in experiments [1]).

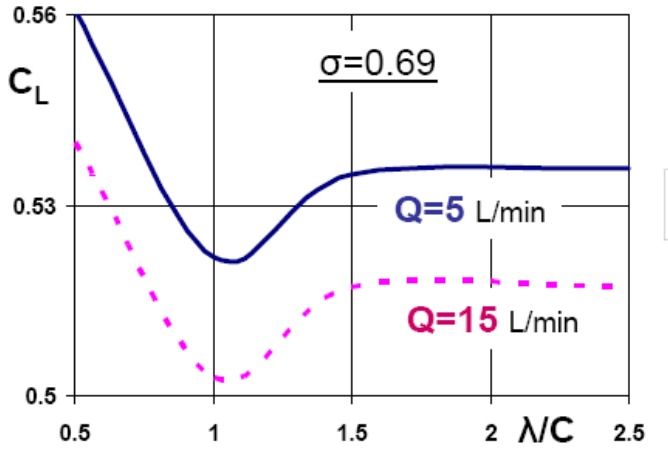

Figure 15: Combined effect of wavelength and air supply on the lift coefficient for an off design condition

ANALYSIS OF SCALE EFFECTS

The flow parameters for ventilated hydrofoil/bodies in applications to engineering will be different from the varied in the water tunnel experiments [1]. The speed increase from 8m/s up to much higher values significantly changes the lift coefficients of the ventilated hydrofoil at off-design conditions only (as shown in Fig.16 for the lift coefficient RMS). Two similar curves for design condition would practically coincide in a plot of the same size.

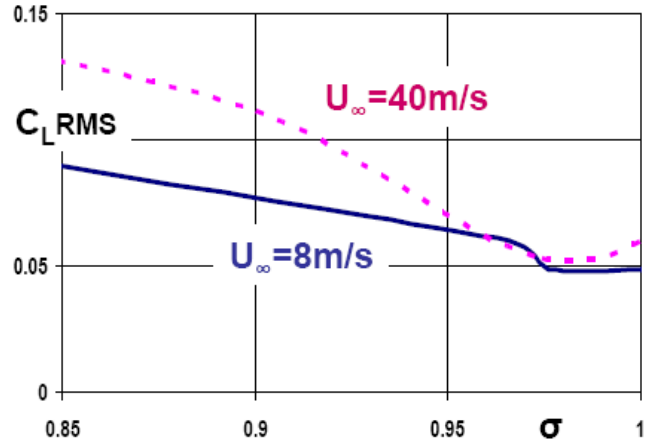

Figure 16: Free stream speed effect on lift pulsation at α=6°

Further, the above-presented results relate to one-frequency (wavelength) and constant amplitude waves which are frequently named as regular. The real sea waves are irregular: They have a range of wavelengths and a range of amplitudes. This irregularity can significantly affect the lift behavior, as is illustrated by Fig.17 for the off-design condition. However, it is interesting to note that the lift RMS in irregular waves is generally lower than it is in regular waves. There is also seen the U_∞ effect in Fig.17. Again, it will be much smaller at the design condition.

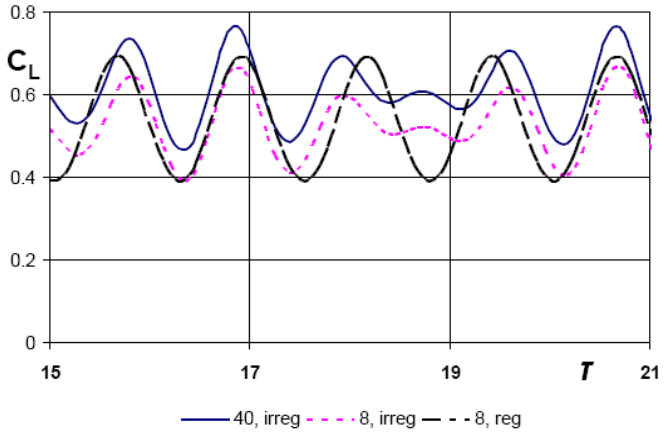

Figure 17: Lift coefficient evolutions in regular and irregular waves for σ=0.78 and α=6°. The numbers in the legends indicate the speed value (in m/s). The regular wave has λ=2.5C, the irregular waves of the same total magnitude are combined from two waves of different lengths.

CONCLUSION

1. A new flow model for ventilated cavitation in unsteady incoming flows is suggested. This model provides coupling of the water flow out of the cavity with the air flow within the cavity. The response of the ventilated hydrofoil to wavy (unsteady) flow excitations is considered as the unsteady perturbation of the steady cavitating flow. Though nonlinear ideal fluid theory has been employed for obtaining the unperturbed steady solution in the presented computations, it was pointed out that another theory may be also employed to create such unperturbed solution.

2. A highly efficient numerical algorithm for the suggested model is developed. The flow model and algorithm was successfully validated with the currently available experimental data for the ventilated hydrofoil OK-2003 in gust flow. Computational dependencies for the average lift and lift pulsation are close to the measured data.

3. The numerical analysis was first applied to estimation of influences of uncertainties in experiments with unsteady cavitation under wave impact. For the conditions of the water tunnel experiments [1], it becomes possible to conclude that:

- Gust induces some very secondary oscillations of the cavitation number;
- Uncertainty of information on the actual water concentration in the cavity is not important at least at the design condition of the low-drag ventilated hydrofoil/bodies.

4. For the hydrofoils (bodies) with ventilated cavities in concavities (niches), the provided numerical analysis manifested that:

- In design conditions, the ventilated cavities in the hydrofoil (body) are substantially stable under wavy excitations (in comparison with off-design conditions).
- Variations of air supply are less influent for the design condition than for other conditions are. An oversupply of air significantly amplifies pulsations at off-design conditions, but its effect at the design condition is not significant.

5. The influence of the real sea conditions (of various wavelengths, irregular wave spectrum and higher flow speeds) on the lift and lift pulsations was also numerically analyzed. It was found that:

- The waves of wavelength equal to the hydrofoil chord have the most significant impact on the ventilated hydrofoil characteristics.
- The difference between hydrofoil response at design and off-design conditions to the impact of waves is quite small for this specific length.
- Air compressibility effect on the force pulsation (due to speed increase) is significant at off-design conditions only.

ACKNOWLEDGMENTS

Author appreciates NAVSEA support of this study (under contract N0002407C4113). Author is also thankful to R.E.A. Arndt and J. Kopriva for the experimental study of the cavitating hydrofoil OK2003 (already reported in [1], [12] and again employed in this paper).

NOMENCLATURE

A=wave magnitude
C=hydrofoil chord
C_D=drag coefficient
C_L=lift coefficient
C_{LRMS} =RMS of lift coefficient
c=sound speed in air
dt=time step
H=cavity thickness
h=perturbation of H
$J = \rho_0 c^2 / \rho_w U_\infty^2$
l_C =cavity length
m=air mass concentration within the cavity
N=normal to S
Pc=cavity pressure
Q=volumetric air flux from the cavity
Q_{sm}=minimum air escape to the cavity boundary layer in a steady flow
q=source-sunk intensity (density of φ)
q*= source-sunk intensity (density of Φ*)
S=inviscid flow boundary
S*=unperturbed cavity surface
Sw=surface of the vortex sheet behind the foil
T=tangent to S
U=gradΦ_0
U_∞ =free-stream speed
u/=tangent component of wave-induced velocity
u_a =depth-averaged longitudinal air velocity in the cavity
V=unperturbed cavity volume
v = normal component of incoming wave velocity
X_1 =cavity detachment abscissa
Γ=vortex intensity
γ= vortex intensity perturbation
ρ' = perturbation of air density normalized by ρ_0
ρ_0 =initial medium density in the cavity
ρ_w =water density
σ = cavitation number
$\tau = tU_\infty / C$ =dimensionless time
Φ and Φ* =velocity potentials
φ=perturbation velocity potential
ψ =incoming wave potential
λ=wavelength
ω=wave frequency

REFERENCES

[1] Kopriva, J., Amromin, E.L and Arndt, R.E.A. 2008 "Improvement of Hydrofoil Performance by Partial Ventilated Cavitation in Steady Flow and Periodic Gusts". *Journal of Fluids Engineering*, v130

[2] Reichardt, H. 1946 "The Law of Cavitation Bubbles at Axially Symmetric Bodies in a Flow" *Reports and Translations, 766,* Ministry of Aircraft Production, UK.

[3] Basin, A., Butuzov, A., Ivanov, A., Olenin, Y., Petrov, V., Potapov, O., Ratner, E., Starobinsky, V. and Eller, A. 1969 "Operational tests of a cargo ship 'XV VLKSM Congress' with air injection under a bottom*". River Transport*, pp52-53

[4] Gowing, S and Shen, Y. 2006 "Ventilation effects on cavitating wedges and struts" *WMTC-2006*, UK

[5] Brennen, C.E. 1969 **"**A numerical solution for axissymmetric cavity flows*". J. Fluid Mechanics*, v37, pp 671

[6] Lorber, P.F. and Covert, E. E. 1982 "Unsteady Airfoil Pressure Produced by Aerodynamic Interference". *AIAA Journal,* v20, pp1153-1159

[7] Nigmatulin, R.I. 1991 *Dynamics of Multiphase Media*. Taylor & Francis

[8] Kinzel, M.P., Lindau, J.W., Peltier, J., Zajaczkowski, F., Arndt, R.E.A., Wosnik, M. and Mallison, T. 2007 "Computational Investigation of Air Entrainment, Hysteresis and Loading for Large-Scale, Buoyant Cavities." *NMSH2007 Conf.*, Ann Arbor, v3, p306

[9] Dubrovsky, V.A., Matveev, K.I. and Sutulo, S. 2007 *Small Waterplane Area Ships*. Blacbone Publ., NJ.

[10] Lang, T.G. and Daybell, D.A. 1961 "Water tunnel Tests of Three Vented Hydrofoils in 2D flow". *J. of Ship Research*, v5, pp1-15

[11] Schiebe, F.R. and Wetzel, J.M. 1964 *Further Studies on Ventilated Cavities of Submerged Bodies*. SAFL Report N72, University of Minnesota

[12] Ando, J., Maita, S. and Nakatake, K. 1998 "A method to calculate characteristics of supercavitating propeller making use of 2-D theory for cavitating wing". *Proceedings of Third International Symposium on Cavitation*, Grenoble, France, v1, pp285-290

[13] Yamaguchi, H. and Kato, H. 1983 "Non-linear theory for partially cavitating hydrofoils". *J. Soc. Naval Arch. Jap*, v152, pp117-124

[14] Kopriva, J., Amromin, E.L., Arndt, R.E.A., Kovinskaya, S.I. and Wosnik,M. 2007 "High performance partially cavitating hydrofoils", *Journal of Ship Research*, v51, pp313-325

[15] Ulhman, J.S. 1987 "The surface singularity method applied to partially cavitating hydrofoil". *J. Ship Research*, v31, pp107-124